

Possible Protective Effect of Bone Marrow-Mesenchymal Stem Cells (BM-MSCs) Against the Remote Liver Injury Induced by Renal Ischemia Reperfusion in Male Albino Rats

Nashwa Fathy Gamal El-Tahawy^{1*} and Abdel Hamid Sayed AboBakr Ali²

¹Department of Histology and Cell Biology, Faculty of Medicine, Minia University, Minia, Egypt

²Department of Anatomy, Faculty of Medicine, Minia University, Minia, Egypt

Abstract

Background: Renal ischemia-reperfusion injury (IRI) is a major cause of acute renal injury and leads to multi-organ dysfunction especially liver injury. Stem cell therapy has been used effectively in treatment of renal IRI.

Aim of the work: To investigate the possible therapeutic effect of BM-MSC therapy on the remotely affected liver in a rat model of renal IRI and the mechanisms involved in this effect.

Methods: Rats were divided into 3 groups; the sham-operated control group, the renal IRI group: bilateral renal IRI for 45 minutes followed by reperfusion, and BM-MSCs-injected group: rats were subjected to renal IRI and then received a single intravenous (iv) injection of BM-MSCs immediately after reperfusion. At the different time-points (days 1, 3, and 5) of the study, serum urea, creatinine, alanine aminotransferase (ALT), and aspartate aminotransferase (AST) were estimated. Livers were removed and were divided: some specimens were homogenized for assessment of oxidant and antioxidant parameters, and other specimens were used for paraffin embedding for histological and immunohistochemical study.

Results: Renal IRI resulted in a significant increase in serum levels of urea, creatinine, AST, ALT, and hepatic tissue levels of malondialdehyde (MDA) which attenuated on days 3 and 5 after BM-MSCs injection. MDA showed an early significant decrease in the BM-MSCs-injected group at day 1. Reduced glutathione (GSH) showed a significant decrease in the IRI sub-groups while BM-MSCs-injected sub-groups showed significantly higher levels of GSH on days 1, 3 and 5. Tissue sections showed that labeled BM-MSCs were engrafted into liver tissue. The IRI subgroups showed marked destruction of liver tissue e.g. disrupted lobular architecture, marked hepatocellular ballooning and cytoplasmic vacuolations, and marked recruitment of the inflammatory cells with vascular congestion. While in the BM-MSCs-injected subgroups, there were gradual regeneration and restoration of lobular architecture, reduced degenerated cells, decreased congestion, and minimal inflammatory cell infiltration. By day 5, most hepatocytes had more or less normal appearance, arranged in cords with preserved general architecture and lacking evidence of major morphological injury. In addition, BM-MSCs significantly attenuated the liver immunohistochemical expression of tumor necrosis factor-alpha (TNF- α).

Conclusion: BM-MSCs protects against the remote liver injury induced by renal IRI through early inhibition of inflammatory cell recruitment, inflammatory reactions, suppressing oxidative stress and lipid peroxidation, and rapid restoration of cellular and architectural integrity of the liver. This provides another important basis for the therapeutic concept of BM-MSCs in treatment of renal IRI by adding a beneficial effect on decreasing the remote liver injury besides considering it as a promising treatment in renal IRI.

Keywords: Remote liver injury; Renal ischemia reperfusion; Mesenchymal stem cells; immunohistochemistry; TNF- α

Introduction

Liver and kidney are both important regulator organs in our body and any liver or kidney injury may influence the other [1]. Acute kidney injury and ischemic renal diseases are common clinical entities [2]. Renal Ischemia-reperfusion injury (IRI) describes the tissue ischemia with an inadequate oxygen supply followed by reperfusion which initiates a wide array of inflammatory responses [3]. Remote organ injury is an oxidative damage that may be seen in various organs away from the tissue exposed to IRI [4]. Remote organ failure like liver, brain and lung commonly coexists with acute renal injury in the intensive care units and it increases the mortality risk [2,5,6]. Despite the advanced renal replacement therapy, mortality among patients who sustain acute renal injury complicated by multiorgan dysfunction, remained unchanged and was estimated at approximately 50% [2].

The identified mechanisms for remote organ affection involved: systemic inflammatory changes, activation of apoptosis, increase of

leukocyte trafficking, and induction of remote oxidative stress [6]. Renal IRI decreases antioxidant enzyme activities [7] and increases neutrophils and lymphocytes accumulation in liver tissue [5]. Furthermore, it causes an increase in inflammatory cytokines like tumor necrosis factor-alpha (TNF- α) [7], and also promotes oxidative stress and lipid peroxidation [8], which in turn causes hepatic structural and

***Corresponding author:** El-Tahawy NFG Assistant Professor, Department of Histology and Cell Biology, Faculty of Medicine, Minia University, Minia, Egypt, Tel: 02/01145435777; E-mail: nashogo@yahoo.com

Received October 01, 2017; **Accepted** November 05, 2017; **Published** November 13, 2017

Citation: El-Tahawy NFG, Ali AHSA (2017) Possible Protective Effect of Bone Marrow-Mesenchymal Stem Cells (BM-MSCs) Against the Remote Liver Injury Induced by Renal Ischemia Reperfusion in Male Albino Rats. J Cytol Histol 8: 484. doi: [10.4172/2157-7099.1000484](https://doi.org/10.4172/2157-7099.1000484)

Copyright: © 2017 El-Tahawy NFG, et al. This is an open-access article distributed under the terms of the Creative Commons Attribution License, which permits unrestricted use, distribution, and reproduction in any medium, provided the original author and source are credited.

functional derangements and cell death ultimately [9]. This complex pathophysiology resulting from a number of contributing factors, so it is difficult to achieve effective treatment or protection by targeting only individual mediators or mechanisms despite the efforts made to deal with this problem [10]. The increasing mortality rate in cases with acute renal injury necessitates designing strategies to assess the effect of renal injury on distant organs [11]. Therefore, several studies [8,1-14] tried to protect liver from remote injury induced by renal IRI for the prevention and attenuation of acute renal injury related morbidity.

Mesenchymal stem cells (MSCs) are emerging as a potential cell therapy for various inflammatory diseases giving much promise for kidney repair after damage [4]. Although the mechanism of MSCs affects remains unclear, their early protection is primarily mediated through complex paracrine actions as immunomodulation and growth factor secretion [15]. Recent studies have shown that transplantation of MSCs in renal IRI in animal models [16-19] or humans [20-22] with renal IRI promotes renal functional recovery and reduces renal tissue damages. This indicates that cell therapy could be a promising alternative treatment for tissue repair and preventing IR-induced renal damage [18]. However, its therapeutic effects on the remotely affected organs induced by renal IRI, was not yet investigated. Therefore, the aim of this study was to investigate the possible therapeutic effect of BM-MSCs therapy on the remotely affected liver in a rat model of renal IRI and the mechanisms involved in this protection which monitored by chemical histological and Immunohistochemical studies.

Material and Methods

Ethics

All aspects of animal care and treatment were carried out according to the local guide-lines of the Ethical Committee of Faculty of Medicine of Minia University.

Bone marrow derived-mesenchymal stem cells (BM-MSCs)

Rat bone marrow derived, bromouridine-labeled, mesenchymal stem cells (BM-MSCs) were purchased from the Nile Center Laboratory Animal Unit of Mansoura Experimental Research (Mansoura, Egypt).

Preparation of BM-MSCs

After anesthetizing rats (6-weeks-old male albino rats) by halothane and skin sterilization, femurs and tibiae of rats were dissected, and washed in Petri dish by phosphate buffer saline (PBS) (Hyclone, USA). Bone marrow was collected by flushing femurs and tibiae with Dulbecco's modified Eagles medium (DMEM) (lonza, Belgium) supplemented with 10% fetal bovine serum (FBS) (lonza, Belgium) and 1% penicillin-streptomycin (lonza, USA). Nucleated cells were isolated using a Ficoll/Paque density gradient (Pharmacia) and were cultured in 20 ml complete media (lonza, USA) supplemented with 1% penicillin-streptomycin and incubated at 37°C in 5% humidified CO₂ incubator (shellab, USA) for 7-10 days until formation of large colonies. The cultured cells were examined daily using the inverted microscope (Olympus CKX41, USA) to follow up the growth of cells. The 2nd exchange for media was done after 3-4 days. The cells took 3-4 weeks to be confluent (80~90% confluence) and be ready for passaging. The media changed twice a week. The culture was washed with PBS and cells were trypsinized with 1-2 ml of 0.25% trypsin in 1 mM EDTA (lonza, Belgium) (5 min at 37°C). Then, 5 ml complete media was added to stop trypsinization, and to test cell. After centrifugation, the cells were resuspended with complete medium in 2 tissue culture flasks (Falcon) containing 15 ml complete media and incubated in humidified

incubator at 37°C in 5% CO₂. BM-MSCs in culture were characterized by their adhesiveness and fusiform shape [23]. Counting of cells were done and number of cells/ml=4 × 10⁵.

Labeling of stem cells

BM-MSCs were harvested during the 2nd passage. Cells were centrifuged and washed twice in serum free medium. Cells were suspended in bromouridine (Sigma Aldrich, Egypt) fluorescent linker dye solution for labeling [23].

The Experimental Design

This study was carried out on 54 adult male Wistar albino rats, weighing 200-250 gm, and of 12 weeks of age. The animals were obtained from Minia University Laboratory Animal House, then housed in plastic cages at room temperature with normal light/dark cycles. Rats were fed a standard laboratory diet and water ad libitum. Animals were randomly divided into three equal groups (18 rats/group):

- i. Group I; the sham-operated control group: rats underwent the same surgical procedure of renal IRI, except that the kidneys were exposed but not clamped. Rats received a single intravenous (iv) injection of saline as a vehicle [12].
- ii. Group II; the renal IRI group: rats were subjected to bilateral renal IRI, then received a single iv injection of saline immediately after reperfusion.
- iii. Group III; BM-MSCs injected group: rats were subjected to bilateral renal IRI, then received a single iv injection of BM-MSCs immediately after reperfusion.

Rats from each group were subdivided into 3 sub-groups (6 rats each) and were sacrificed as follows:

1. Sub-group a: 1 day after saline or BM-MSCs injection.
2. Sub-group b: 3 days after saline or MSCs injection.
3. Sub-group c: 5 days after saline or BM-MSCs injection.

Induction of experimental Renal IRI

Rats were placed on a warming pad and were anesthetized with pentobarbital sodium (60 mg/kg i.p). A midline abdominal incision was performed after disinfection, kidneys were exposed, and renal pedicles were bilaterally clamped by non-traumatic clamps for 45 minutes, followed by reperfusion by removal of the clamps [24]. The occlusion and reperfusion were verified visually by changes in color. The incisions were covered with gauze soaked with normal saline to prevent evaporation. Body temperature was maintained at 37 ± 1°C. The incision was closed in 2 layers and a topical application of garamycin cream was used to avoid wound infection.

Injection of BM-MSCs

Immediately after assurance of renal reflow, rats of group III received 0.5 ml bromouridine-labeled BM-MSCs (2 × 10⁵) diluted with 1 ml saline, loaded in a 1-ml sterile syringe and injected intravenously in the tail vein for each rat [19].

Animal sacrifice and tissue obtaining

At the end of the experiment, 6 rats of each sub-group at each time point were sacrificed by decapitation after light ether anesthesia. Tail vein blood samples were collected shortly prior to scarification.

Livers were rapidly removed and were divided; some specimens were placed into liquid nitrogen and then stored at -70°C until assayed for oxidant and antioxidant parameters, and other specimens were used for paraffin embedding.

Biochemical Assay

Determination of renal and liver functions

Tail vein blood samples were collected shortly prior to IRI induction (at day 0 for exclusion of renal or hepatic abnormal functions) and after intervention throughout the experiment at day 1, day 3 and day 5. Sera were used for estimation of: urea by Berthelot enzymatic colorimetric method, creatinine by Jaffé calorimetric-end point method [25] as renal function tests. Liver transaminases; alanine aminotransferase (ALT) and aspartate aminotransferase (AST), by the enzymatic colorimetric methods [26] using commercial kits (Biodiagnostic, Egypt).

Determination of lipid peroxidation; malondialdehyde (MDA), and the antioxidant enzyme; reduced glutathione (GSH)

Liver tissues were homogenized in 1:10 (wt:vol) phosphate buffer (pH 7.4) by the use of a Teflon headed homogenizer at a speed of 2500 rpm. Triton x100 and protease inhibitor cocktail were added. The homogenates were centrifuged at 6.000g for 10 min at 4°C . The resulting supernatant was used for colorimetric determination of hepatic MDA [27] and GSH [28] using commercially available kits (Biodiagnostic, Egypt) using the spectrophotometer (Jenway 7305, Staffordshire, UK).

Histological procedures

Liver specimens were fixed in 10% buffered formalin, followed by paraffin embedding. Some sections of 5~7 μm thickness were cut, mounted on glass slides and stained with hematoxylin and eosin (H&E) for histological examination [29].

Immunohistochemistry

Other 5 μ -sections were used for immunohistochemical staining for the mouse monoclonal TNF- α (Sigma Aldrich, Egypt) according to the manufacture's guidelines. Briefly, sections were deparaffinized, rehydrated, incubated with 0.1% trypsin and 0.1% $\text{CaCl}_2 \cdot 2\text{H}_2\text{O}$ in 50 mM Tris buffer at pH 7.4 at 37°C for 120 minutes, and soaked in absolute methanol containing 0.3% hydrogen peroxid for 30 min at room temperature. Sections were then incubated with 1.5% non-immunized goat serum for 30 min, then incubated with the diluted TNF- α antibodies (5-10 $\mu\text{g}/\text{ml}$) for 30 minutes at room temperature, and washed 3 times with phosphate-buffered saline (PBS) for 30 min. Thereafter, sections were incubated for 60 min with biotinylated goat anti-mouse Ig serum. Sections were washed with PBS and incubated with avidin/biotin peroxidase complex (Vector, Burlingame, CA). Sites of peroxidase binding were detected using chromogenic 3,3'-diaminobenzidine (DAB) tetra hydrochloride substrate. Tissue sections were counterstained with haematoxylin. Positive cells showed brown cytoplasmic reaction [30].

Positive tissue control

Sections of human tonsil were immunostained for TNF- α .

Negative control

Other sections of liver in the sham-operated control group were processed in the same way but skipping the step of applying the primary antibody (figures not included).

Image capture

a) For detection of engraftment of bromouridine-labeled BM-MSCs in the liver tissue, H&E sections were examined using a fluorescence microscope (Leica M205 FCA, Germany).

b) H&E and immunostained sections were examined using a light microscope (Olympus, Japan). Images were digitally captured using a hardware consisting of a high-resolution color digital camera mounted on the microscope, connected to a computer.

Morphometric study

The TNF- α immunopositive cells were counted in 10 adjacent non-overlapping fields of the tissue sections of each rat in all sub-groups [30].

Data handling and statistics

Analysis of the quantitative data was carried out using SPSS version 20 (SPSS Inc., Chicago, Illinois, USA). Data were represented as mean \pm standard deviation (mean \pm SD). Significant difference between sub-groups was done by one-way ANOVA followed by Tukey-Kramer post hoc test for multiple comparisons. p -value ≤ 0.05 considered statistically significant.

Results

Effect of BM-MSCs on renal and hepatic function tests

Renal ischemia-reperfusion injury (IRI) resulted in a significant increase in serum urea, creatinine, aspartate aminotransferase (AST) and alanine aminotransferase (ALT), levels on days 1, 3 and 5 compared with those in sham-operated control rats (all $p = 0.000$). Their levels in the BM-MSC group on day 1 showed no significant difference compared to the IRI group (all $p > 0.05$). On days 3 and 5, the levels showed significant decrease compared with the IRI group (all $p \leq 0.05$) but it was still showed a significant difference with the sham-operated control group (all $p \leq 0.05$) (Table 1).

Effect of BM-MSCs on renal IRI-induced oxidative stress in the liver evaluated by malondialdehyde (MDA) and reduced glutathione (GSH) levels

Hepatic tissue levels of MDA were significantly higher in the IRI group on days 1, 3 and 5 compared with those in sham-operated control rats (all $p = 0.000$). BM-MSCs-injected group showed an early significant decrease in the MDA levels at day 1 and also at day 3 and 5 (all $p = 0.000$) compared with the IRI sub-groups, but remained significantly elevated compared to the sham-operated control group (all $p \leq 0.05$) at the corresponding time points.

Regarding the hepatic tissue levels of GSH there was a significant decrease in IRI sub-groups compared to the sham-operated control rats on days 1, 3 and 5 (all $p = 0.000$). However, the BM-MSCs-injected sub-groups showed significantly higher levels on days 1, 3 and 5 (all $p = 0.000$) compared to IRI sub-groups, but still there was a significant difference when compared with the sham-operated control group at the day 1 and 3 (all $p \leq 0.05$) with an insignificant difference at day 5 ($p = 0.26$) (Table 2).

Histological findings in hepatic tissues

Confirmation of homing of BM-MSCs into the liver tissue: Bromouridine-labeled BM-MSCs showed green auto fluorescence after transplantation into rats in the BM-MSCs-injected sub-groups, confirming that these cells were engrafted into liver tissue. Sections in

Values	Sham-operated control group	IRI group	BM-MSCs-injected group	p-values		
				p1	p2	P3
Serum urea (mg/dl)						
Day 1	30.17 ± 0.48	98 ± 1.73	93.17 ± 1.60	0.000*	0.078	0.000*
Day 3	30.21 ± 0.31	108 ± 3.39	71.5 ± 1.98	0.000*	0.000*	0.000*
Day 5	29.95 ± 0.94	95.17 ± 2.77	41 ± 2.11	0.000*	0.000*	0.005*
Serum creatinine (mg/dl)						
Day 1	0.83 ± 0.01	2.45 ± 0.01	2.43 ± 0.69	0.000*	0.718	0.000*
Day 3	0.84 ± 0.00	3.16 ± 0.87	2.09 ± 0.67	0.000*	0.000*	0.000*
Day 5	0.81 ± 0.02	2.32 ± 0.05	0.93 ± 0.21	0.000*	0.000*	0.004*
Serum ALT (IU/L)						
Day 1	30.14 ± 1.2	58.96 ± 0.92	56.84 ± 1.17	0.000*	0.074	0.000*
Day 3	30.21 ± 1.17	61.68 ± 0.58	47.89 ± 0.2	0.000*	0.000*	0.000*
Day 5	29.96 ± 1.9	53.52 ± 1.56	38.07 ± 1.63	0.000*	0.000*	0.013*
Serum AST (IU/L)						
Day 1	18.02 ± 0.35	27.90 ± 0.39	24.71 ± 1.18	0.000*	0.097	0.003*
Day 3	18.00 ± 0.27	28.17 ± 0.38	21.06 ± 0.31	0.000*	0.000*	0.001*
Day 5	17.95 ± 0.1	27.82 ± 0.42	19.31 ± 0.18	0.000*	0.000*	0.023*

p1: IRI group vs. the sham-operated control group, p2: BM-MSCs-injected group vs. IRI group, and p3: BM-MSCs-injected group vs. the sham-operated control group. *p ≤ 0.05 is significant.

Table 1: Biochemical values in the studied groups at different time points (n=6).

Values	Sham-operated control group	IRI group	BM-MSCs-injected group	p-values		
				p1	p2	p3
MDA (nmol/g tissue)						
Day 1	94.69 ± 0.35	358.35 ± 14.74	138.16 ± 1.3	0.000*	0.000*	0.000*
Day 3	95.07 ± 0.15	374.65 ± 11.43	140.18 ± 1.30	0.000*	0.000*	0.019*
Day 5	91.89 ± 1.61	332.47 ± 12.91	104.79 ± 2.73	0.000*	0.000*	0.053*
GSH (nmol/g tissue)						
Day 1	768.33 ± 14.1	428.67 ± 10.9	653.33 ± 19.13	0.000*	0.000*	0.008*
Day 3	764 ± 18.6	422.83 ± 16.57	705.17 ± 19.27	0.000*	0.000*	0.055*
Day 5	771.01 ± 11.6	427.67 ± 11.01	726.67 ± 13.08	0.000*	0.000*	0.26

p1: RI group vs. the sham-operated control group, p2: BM-MSCs-injected group vs. IRI group, and p3: BM-MSCs-injected group vs. the sham-operated control group. *p ≤ 0.05 is significant.

Table 2: The tissue levels of MDA and GSH in the studied groups at the different time points (n=6).

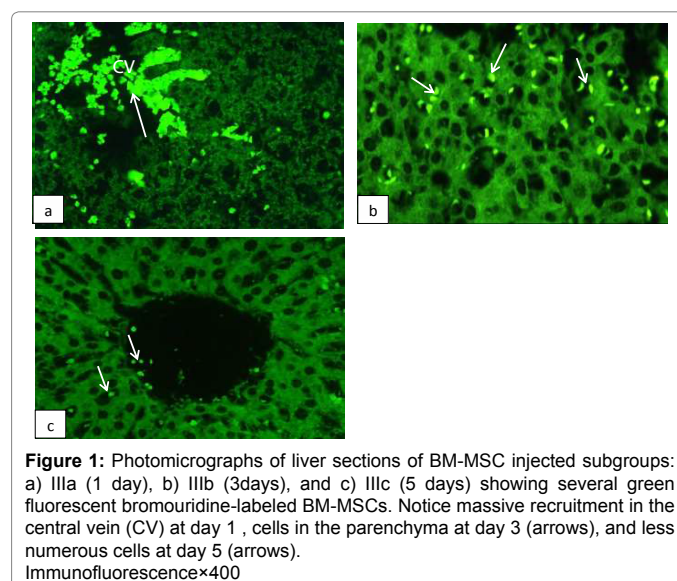
livers of sub-groups IIIa and IIIb showed numerous BM-MSCs labeled with bromouridine with obvious decrease in sub-group IIIc (Figure 1).

Hematoxylin and eosin-stained sections

Liver sections of the sham-control group exhibited normal lobular architecture at the different time-points of the experiment (represented in Figure 2). Hepatocytes radiated from the central vein forming anastomosing fenestrated plates separated by the hepatic sinusoids. Portal tracts contained branches of portal vein, hepatic artery, and bile duct. The hepatocytes appeared polyhedral with acidophilic finely granular cytoplasm and large central vesicular nuclei with prominent nucleoli. Hepatocytes may be bi-nucleated.

Examination of sections of sub-groups IIa (Figure 3) and IIIa (Figure 4) showed disrupted lobular architecture and marked hepatic injury especially in the periportal areas characterized by marked hepatocellular ballooning and cytoplasmic vacuulations. Their nuclei appeared malformed. Interestingly, sections of sub-group IIa exhibited marked recruitment of the inflammatory cells; neutrophils and lymphocytes, in the vicinity of the portal tract with prominent vascular congestion.

Sub-group IIb showed no obvious changes compared to sub-group IIa. Central vein appeared congested and engorged with inflammatory cells. The inflammatory cells infiltrated the hepatic tissue. Degenerated



hepatocytes with vacuolated cytoplasm and ghosts of nuclei were numerous. Other cells showed apoptotic features in the form of dense nuclei and deeply acidophilic cytoplasm (Figure 5). While sub-group IIIb showed some sort of regeneration e.g. restored lobular architecture

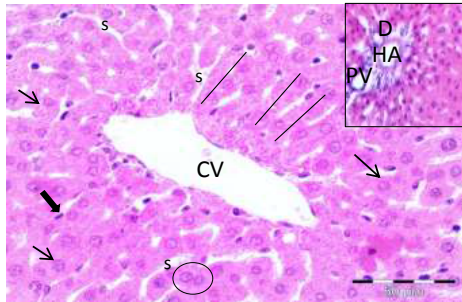


Figure 2: A representative photomicrograph of rat liver tissue from the control group with normal lobular architecture showing: plates (lines) of polygonal hepatocytes with an acidophilic granular cytoplasm and rounded vesicular nuclei (arrows). The hepatocytes are radiating from the central veins (CV) and separated by blood sinusoids (S) lined by endothelium with flat nuclei (thick arrow). Notice binucleated hepatocytes (circle). Inset: portal tract containing branches of the portal vein (PV), hepatic artery (HA), and bile duct (D). H&E $\times 400$.

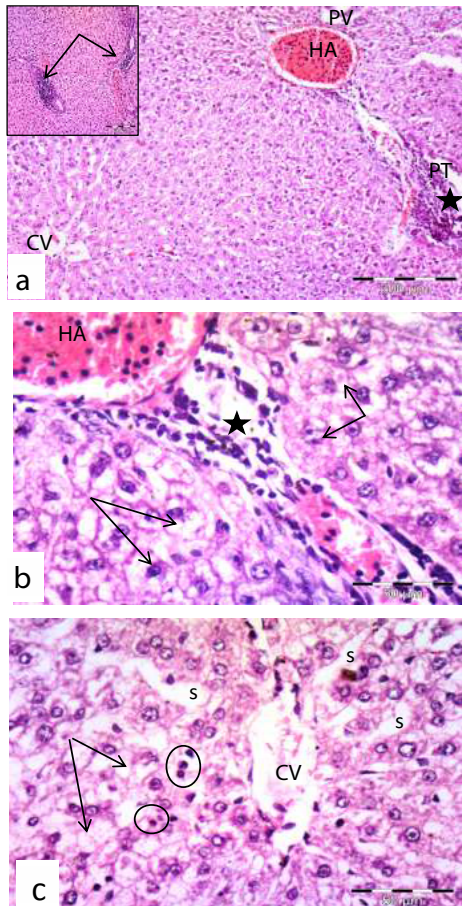


Figure 3: Photomicrographs of rat liver tissue from group IIa showing:
a) Loss of lobular architecture with massive recruitment of inflammatory cells (star and arrows in inset) around the portal tract (PT). Notice Congestion and apparent dilatation of hepatic artery (HA), and less affection of hepatocytes surrounding the central vein (CV).
b) Ballooned hepatocytes with foamy vacuolated cytoplasm and deformed nuclei (arrows) in the portal area (PT). Congestion and engorgement of hepatic artery (HA) with inflammatory cells.
c) Sinusoidal dilatation (s) around central vein (CV). Note scattered inflammatory cells; lymphocytes and neutrophils (star) between degenerated hepatocytes (arrows).
H&E, a and inset $\times 100$, b and c $\times 400$.

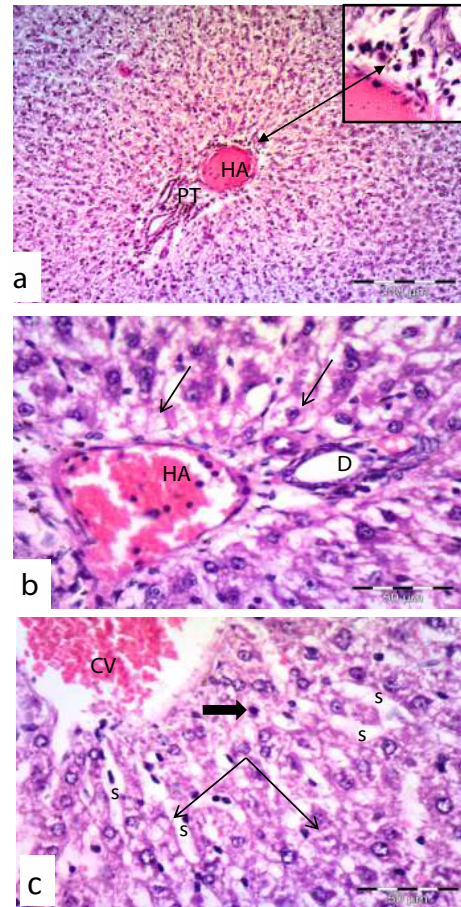


Figure 4: Photomicrographs of rat liver tissue from group IIIa showing:
a) Loss of lobular architecture with minimal inflammatory cells infiltration (arrow and inset) around the portal tract (PT).
b) Congestion of the hepatic artery (HA) with vacuolations of hepatocytes (arrows).
c) Congestion of the central vein (CV), sinusoidal dilatation (s), vacuolations of hepatocytes (arrows), and few cells with dense nucleus and deeply acidophilic cytoplasm (thick arrow). Notice the vacuolated hepatocytes (arrows) are less affected than those surrounding the PT.
H&E, a $\times 100$, inset, b and c $\times 400$.

with less marked degenerative changes in cells, decreased congestion, mildly dilated blood sinusoids, and also minimal inflammatory cell infiltration. Most hepatocytes had more or less normal appearance, arranged in cords with minimal small vacuoles. Few cells with apoptotic features (dense nucleus and deeply acidophilic cytoplasm) were observed (Figure 6).

Sections of sub-group IIc (Figure 7) showed no obvious differences compared to sub-groups IIa and IIb. While sub-group IIIc exhibited marked morphological restoration in the form of preserved general architecture and lacking evidence of major morphological injury. Most hepatocytes restored its cytoplasm without vacuolations and most nuclei appeared normal vesicular with scarcely observed degenerated cells. Vascular congestion appeared to be remarkably reduced. Only mild dilatation of some blood sinusoids, and inflammatory cells were rarely seen (Figure 8).

Immunohistochemical results

Examination of wide fields of sham-operated control group showed no TNF- α immunolabeled cells (Figures 9-14). Extensive

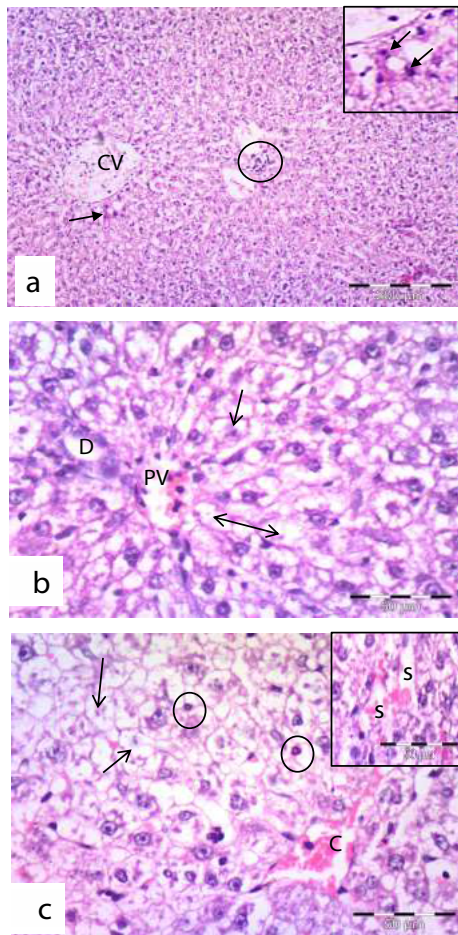


Figure 5: Photomicrographs of rat liver tissue from group IIb showing that: a) Inflammatory cells engorging the central vein (CV) and infiltrating the hepatic tissue (circle). Inset: cells with dense fragmented nuclei and deeply acidophilic cytoplasm (arrows). b) Portal area with apparent dilatation and congestion of the portal vein (PV). Note degenerated hepatocytes with ghosts of nuclei (arrows) or devoid of nuclei (double head arrow). c) Degenerated hepatocytes with vacuolated cytoplasm and ghosts of nuclei (arrows), inflammatory cell infiltration (circles), and vascular congestion (C). Inset: congested dilated sinusoids (s). H&E, a $\times 100$, b, c and insets $\times 400$.

immunolabeling for TNF- α was markedly observed in the liver sections of sub-groups IIa (Figure 10), IIb (Figure 12), IIc (Figure 14), and IIIa (Figure 11). Unexpectedly, sub-group IIIa showed numerous immunolabeled cells in some sections compared to sub-group IIa. Sub-group IIIb (Figure 13) showed some decrease while sub-group IIIc (Figure 15) showed marked decrease in the TNF- α expression when compared to the extensive immunolabeling seen in sub-group IIc. The immunoreactivity for TNF- α was observed in hepatocytes, macrophages (Von-kupffer cells), and endothelial cells. The immunolabeling was cytoplasmic.

Morphometric results

There was a significant increase in the number of TNF- α immunolabeled cells in the IRI and BM-MSCs-injected sub-groups compared to the corresponding sham-operated control group (all $p = 0.000$). While there was a significant decrease in the BM-MSCs-injected sub-groups compared to the corresponding IRI sub-groups (all $p < 0.05$) (Table 3).

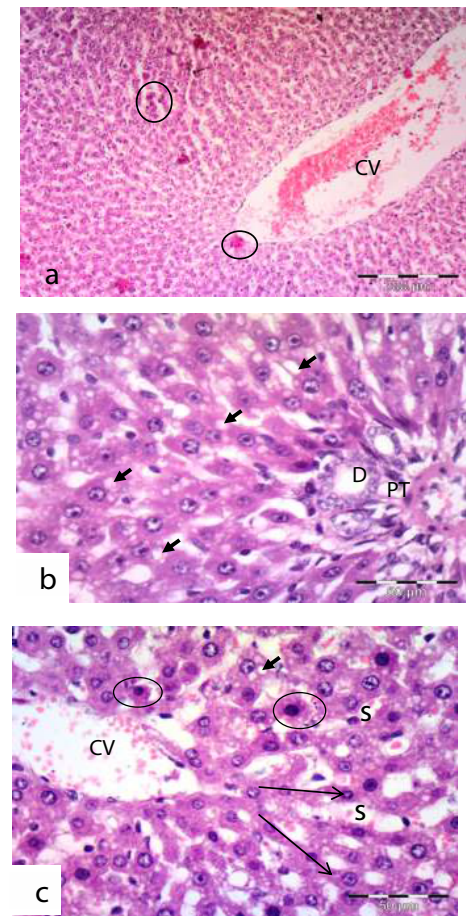
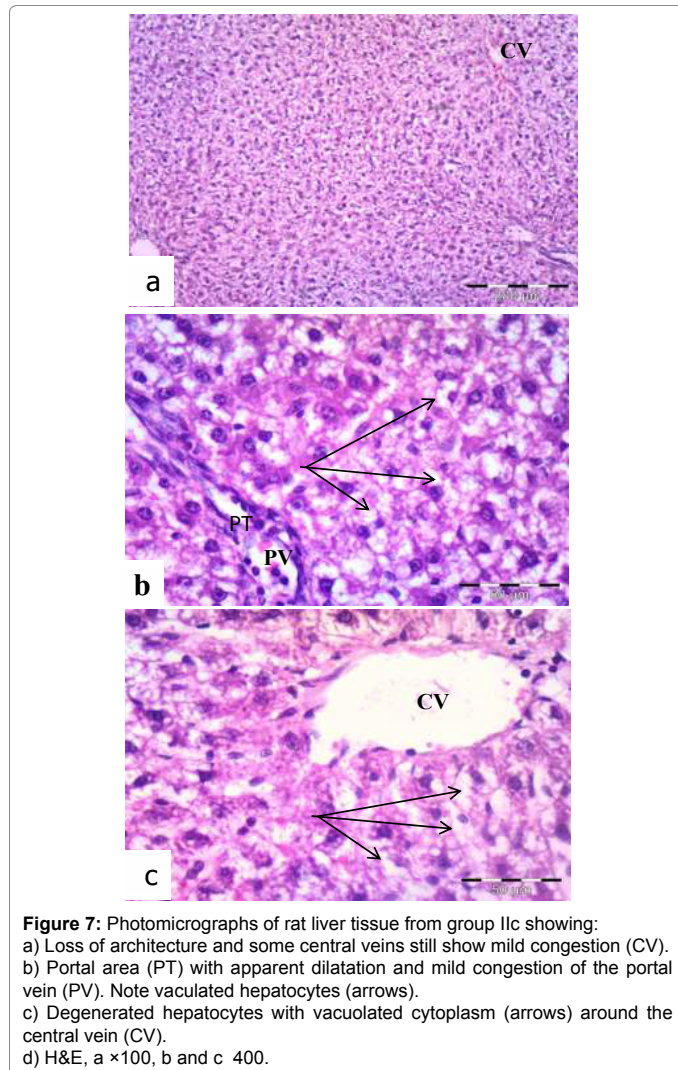


Figure 6: Photomicrographs of rat liver tissue from group IIIb showing that: a) Restored lobular architecture with mild central vein (CV) congestion and scattered areas of degenerations (circles). b) Most hepatocytes with apparent normal appearance, arranged in cords (arrows) with minimal small vacuoles (short arrows). Notice the congested dilated sinusoids (s) and few cells with dense nucleus and deeply acidophilic cytoplasm (circles). c) Portal area (PT) with decreased hepatocyte degeneration. Notice few cytoplasmic vacuolations (arrows). d) H&E, a $\times 100$, b, c $\times 400$.

Discussion

The present study demonstrated that bilateral renal IRI led to damage of the liver as a remote organ. The significant increase in serum urea and creatinine confirmed the occurrence of renal dysfunction and the altered serum AST and ALT indicated remote liver injury. Renal IRI induces an inflammatory response, which results in the formation of reactive oxygen species (ROS) that augments local tissue damage or affects organs remote from the site of IRI [1,5,6,9]. Several previous studies [16-18], suggested that stem cell therapy enhance renal IRI. Also in this study, administration of BM-MSCs-injected resulted in significant improvement of renal functions evidenced by serological results. Moreover, this study proved that administration of BM-MSC also rapidly and gradually restored liver functions evidenced by significant improvement of serum AST and ALT.

Hepatic oxidative stress is evidenced by increased liver MDA; a lipid peroxidation marker [31] and decreased levels of the antioxidant enzyme (GSH) [5,7]. In the present study, a significantly increased

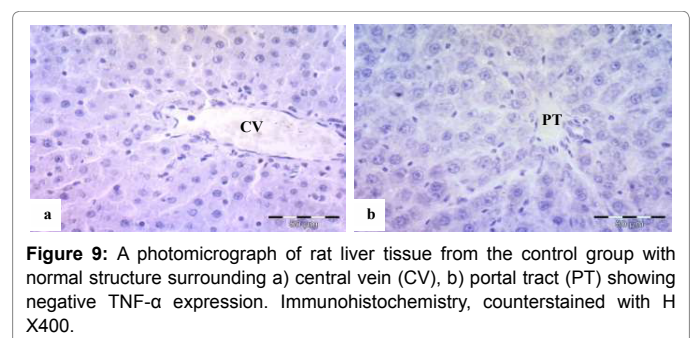
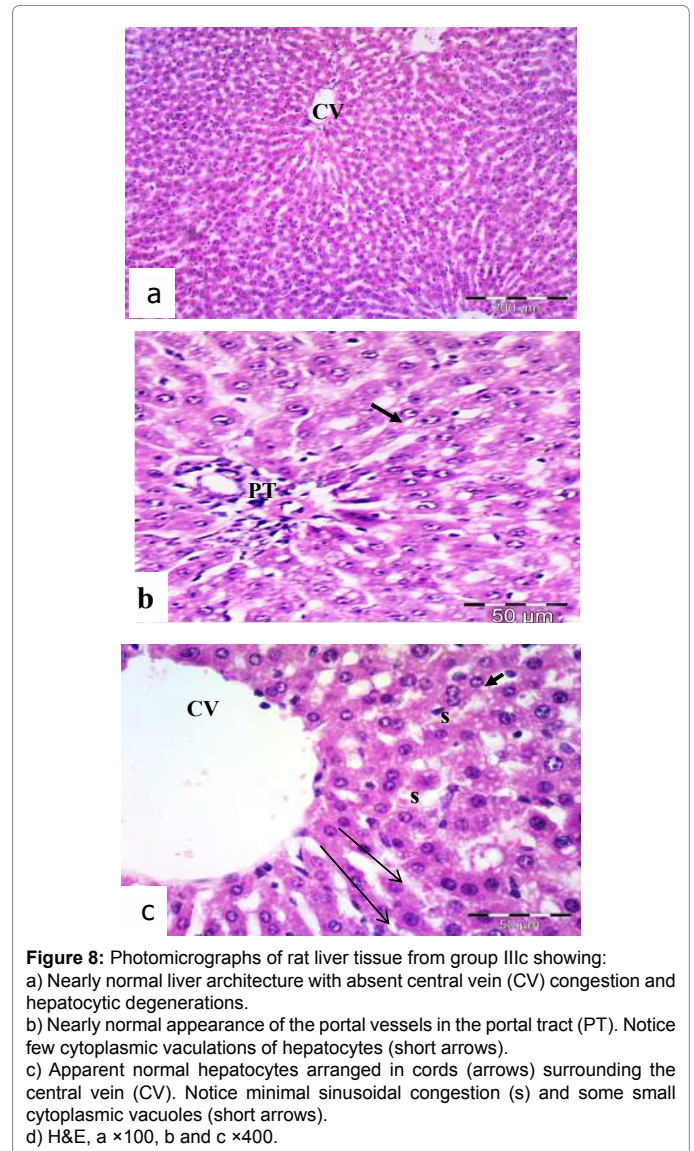


MDA levels and decreased GSH levels reflected the overproduction of ROS generated during ischemia followed by reperfusion, which was then removed by GSH.

Hepatic GSH depletion occurred in the IRI sub-groups might be caused by inhibition of GSH biosynthesis through down-regulation of the trans-sulfuration pathway that limits the availability of cysteine; an essential precursor for GSH biosynthesis as mentioned by Shang et al. [32].

Light microscopic examination of this study showed that altered liver enzymes and changes in hepatic oxidative stress markers were in harmony with the hepatic morphological findings. Renal IRI rapidly caused marked hepatic vacuolization evident sinusoidal dilatation, and vascular congestion. These results were supported by other researchers [1,7] who stated that liver cell injury and hepatocyte death (necrotic and apoptotic) occurred following renal IRI as a result of oxidative stress and decreased its antioxidant capacity. In addition, some investigators attributed liver cell damage to the microvascular reorganization of hepatic parenchyma [33].

ROS causes oxidation of membrane lipids, essential cellular proteins, and DNA leading to release of proteolytic lysosomal enzymes and mitochondrial matrix enzymes into the cytoplasm ending finally in cellular damage [34].



Tissue sections also showed that renal IRI induced massive leukocytic recruitments in liver tissue. This was in a good agreement with several studies [5,7] who reported recruitment and activation of neutrophils as a key step in the development of local and systemic injury in renal IRI.

Another important finding in the current study was the

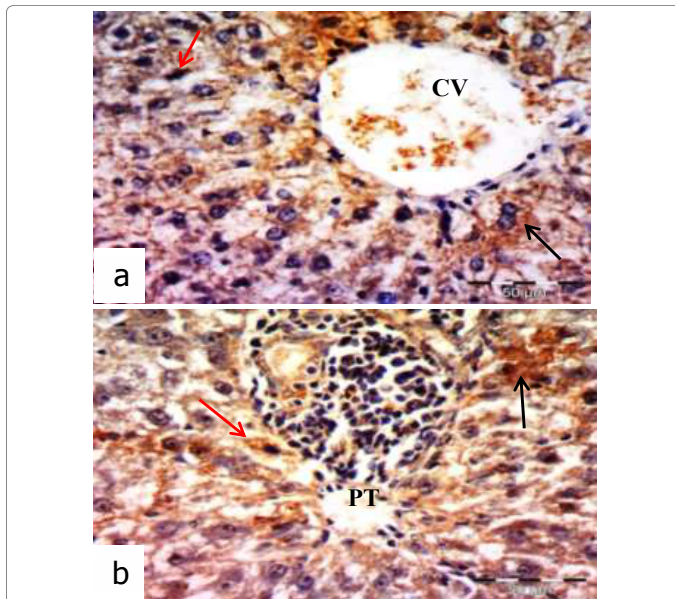


Figure 10: Rat liver tissues immunolabeled for TNF- α in group IIa at: a) central vein (CV), and b) portal tract (PT) showing: extensive immunolabeling of hepatocytes (black arrow) and von-Kupfer cells (red arrow). notice the inflammatory cells infiltrating vicinity of portal tract. Immunohistochemistry, counterstained with H X400.

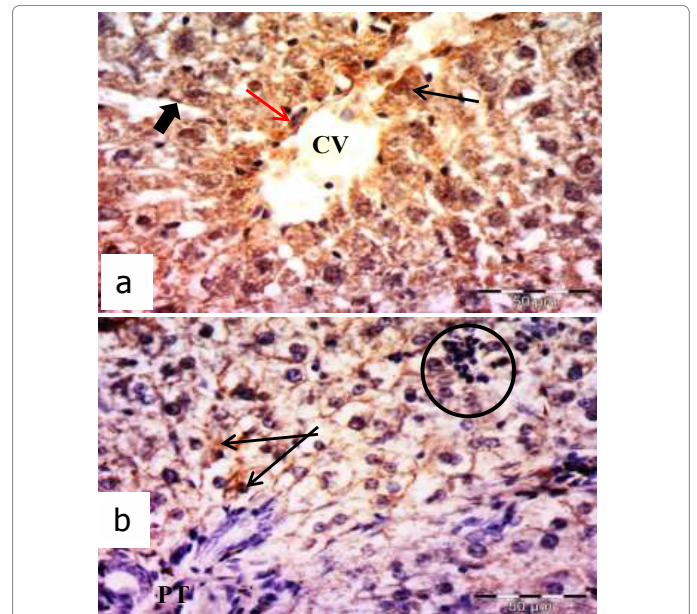


Figure 12: Rat liver tissues immunolabeled for TNF- α in group IIb, showing: a) Extensive immunolabeling of hepatocytes (black arrow), von-Kupfer cells (red arrow), and endothelial cells (thick arrow) around central vein (CV). b) The remnant of the cytoplasm of extensively vacuolated hepatocytes (black arrow) showed immunoreactivity around the portal tract (PT). Notice the inflammatory cells infiltrating between hepatocytes (circle). Immunohistochemistry, counterstained with H X400.

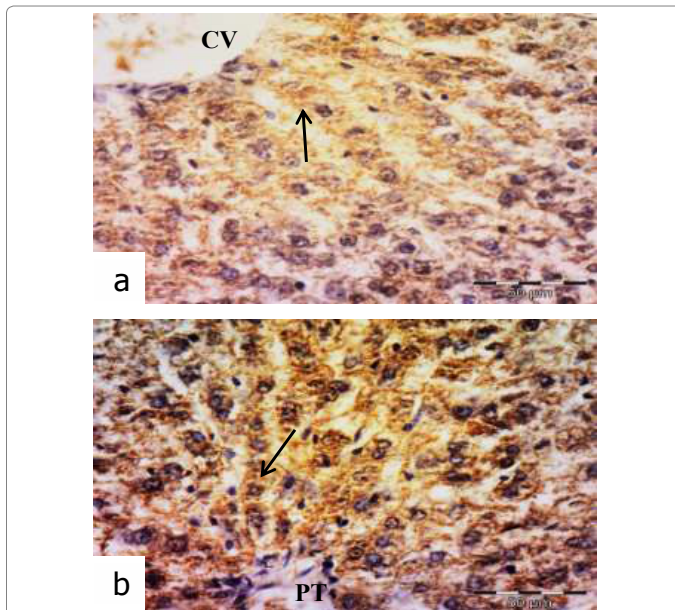


Figure 11: Rat liver tissues immunolabeled for TNF- α in group IIIa, showing: a) immunolabeling of hepatocytes (black arrow), and von-Kupfer cells (red arrow) around: central vein (CV). b) Severely vacuolated hepatocytes with little immunoreactivity (arrows) around the portal tract (PT). Immunohistochemistry, counterstained with H X400.

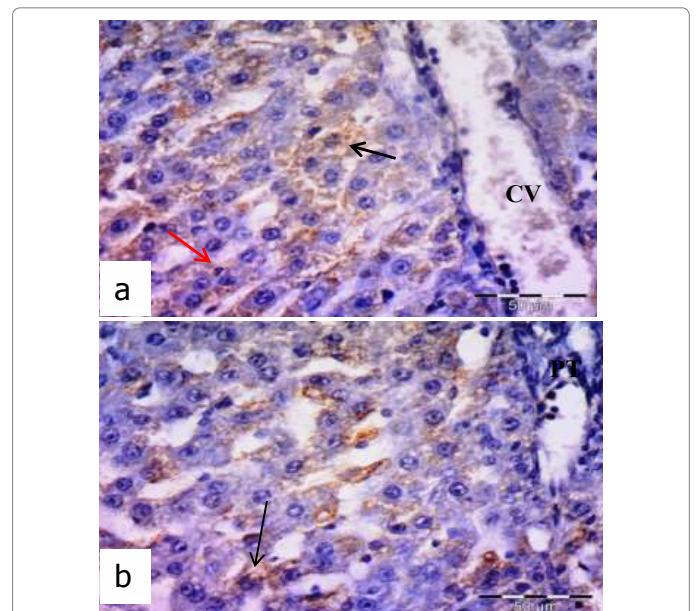


Figure 13: Rat liver tissues immunolabeled for TNF- α in group IIIb, showing decreased immunolabeling of cells; hepatocytes (black arrow) and von-Kupfer cells (red arrow). Immunohistochemistry, counterstained with H X400.

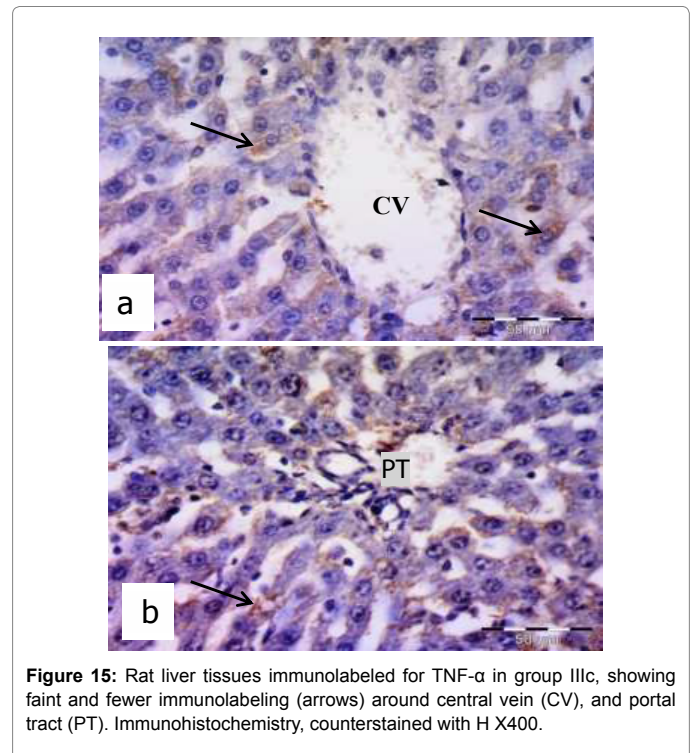
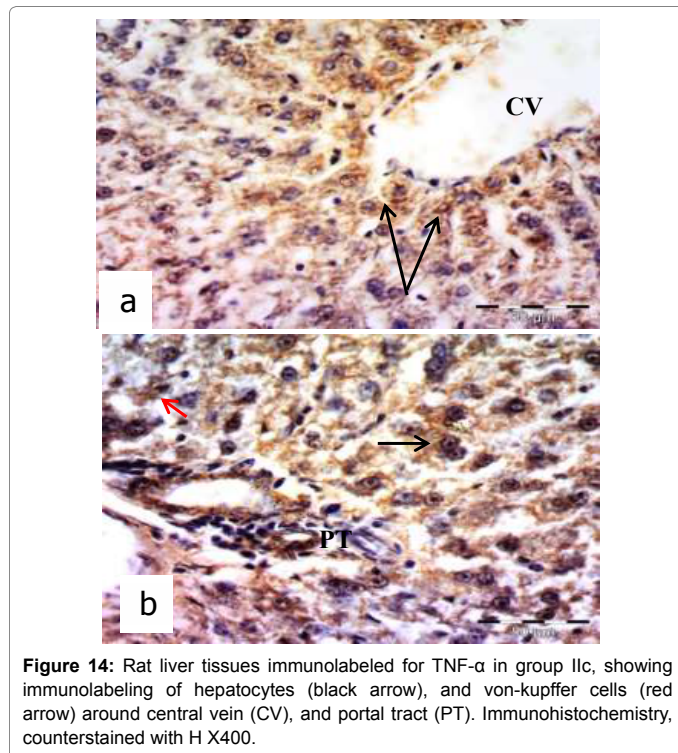
expressions of TNF- α in liver tissues of IRI sub-groups detected by immunohistochemistry. There was marked increase in TNF- α expression in sections of IRI sub-groups compared to sham-operated control group. This was in agreement with those of previous studies [21,35]. TNF- α is a strong early pro-inflammatory mediator that released from a variety of cells (e.g. hepatocytes, Von-Kupfer cells, extra) in response to injury [36]. Renal IRI results in uncontrolled expression of interleukin-17A in the small intestines (1). IL-17A causes

recruitment of neutrophils, activates T cells, and induces expression of other cytokines and chemokines such as TNF- α and IL-6 in liver tissue [11,37]. Moreover, other studies showed that following experimental renal IRI in knockout mice for TNF- α or neutralized with TNF- α antibodies displayed reduced hepatic injury after renal IRI [1]. The overexpression of TNF- α in this study pointed out the severe damage

Values	Sham-operated control group	IRI group	BM-MSCs-injected group	p-values		
				p1	p2	p3
Day 1	0.61 ± 0.2	27 ± 3.8	22.8 ± 0.94	0.000*	0.025*	0.000*
Day 3	0.59 ± 0.1	29 ± 4.6	8.11 ± 1.01	0.000*	0.000*	0.000*
Day 5	0.42 ± 0.5	25 ± 1.3	3.9 ± 0.3	0.000*	0.000*	0.000*

p1: IRI group vs. the sham-operated control group, p2: BM-MSCs-injected group vs. IRI group, and p3: BM-MSCs-injected group vs. the sham-operated control group. *p ≤ 0.05 is significant.

Table 3: Mean number of TNF-α immunolabeled cells in the three groups at different time points (n=6).



observed in the hepatic parenchyma and impairment of liver functions in the IRI sub-groups.

In this study, the injected BM-MSCs migrated to the remotely injured liver in BM-MSCs-injected sub-groups, which was confirmed by localization of bromouridine-labeled BM-MSCs visualized by the fluorescent microscopy. Homing of stem cells to the injured sites could be attributed to certain substances; e.g. chemokine, released at sites of tissue damage at the inflammation site which directs MSCs migration to these sites [20]. MSCs express receptors for several chemokine's such as stromal-derived factor-1, platelet-derived growth factor and CD44 which are likely implicates in regulation of its homing [38]. The migrated MSCs might act by paracrine effects and/or its differentiation [20,39].

Several mechanisms of stem cell therapy which affect the injured tissues had been established which included anti-inflammatory reaction, anti-oxidative stress, stem cell homing and trans-differentiation, and immune-modulation. MSC transplantation limits cellular apoptosis and architectural damage [20,21,40].

Accumulating evidences demonstrated that MSCs contributes to the down-regulation of inflammatory reaction in ischemic condition [41]. In this study, serum ALT and AST levels were reduced in the BM-MSC sub-groups, corroborating the protective effect of BM-MSCs.

Also there was a significant decrease of MDA and a significant increase of reduced GSH. This means that BM-MSC suppressed the oxidative stress and lipid peroxidation induced by renal IRI. The lower level of MDA in the liver tissue at day 1 was indicative of an early protection of BM-MSCs to the liver by reducing the oxidative stress markers and preservation of the antioxidative enzymes with a consequent anti-inflammatory response.

Light microscopic examination of the BM-MSCs-injected sub-groups revealed that during the 1st 24 hours, there was hepatic tissue injury as observed in the IRI sub-groups, but an important observation was the less marked inflammatory cell recruitment. Subsequently, rapid improvement in the histological morphology of the liver observed at day 3 and became more or less as normal by the 5th day. The process of trans-differentiation of administered MSC requires more than 3 days and the early improvement is due to the paracrine effects of stem cells [24]. In this study, the early effects of BM-MSCs were noted within 3 days of injection; before the sufficient time required for cellular growth, division and differentiation. Therefore, direct hepatic parenchymal repopulation by exogenous BM-MSCs is probably a less significant mechanism of BM-MSCs induced hepatic repair. However, the prolonged presence of BM-MSCs in liver and its trans-differentiation remains to be elucidated.

Inflammatory pathway was implicated in the kidney-liver cross-

talk [6]. Giving the importance of inflammation in the pathogenesis of remote liver injury induced by renal IRI, was very important to consider the immunomodulatory properties of BM-MSCs and its role in hepatic protection. In this study, BM-MSCs blocked the hepatic inflammation by inhibiting inflammatory cell recruitments, where minimal inflammatory cells were observed infiltrating the hepatic tissue if compared to massive infiltration of these cells in the IRI sub-group at the different time points of the study. Therefore, this study suggested that BM-MSCs, by its potent anti-inflammatory effects, were protective against renal IRI with subsequent reduced the remote hepatic injury in rats.

Stem cells were able to ameliorate renal IRI in a mouse model via the suppression of TNF- α (18,22). In the current study, administration of BM-MSCs normalized the overexpression of TNF- α in liver tissues. As Von-Kupffer cells play an important role as an initial cytotoxic cell type and are likely to be a source of ROS [42,43] conversely, it may protect the tissues by secretion of anti-inflammatory cytokines [44]. The unexpected apparent increase in the immunolabeled cells in some sections of sub-group IIIa compared to sub-group IIa could be due to the massive vacuulations in cells of sub-group IIIa.

Taken together the findings of the present study beside the advantages of treatment of renal IRI by MSCs which confirmed by several studies [16-19,21,22,40], it could be assumed that treatment of renal IRI with BM-MSCs did not prevent the acute remote liver injury induced by renal IRI but ameliorated this injury and enhanced rapid liver recovery both morphologically and functionally which likely mediated by various paracrine mechanisms distinct from trans-differentiation. This was, at least in part, through early inhibition of inflammatory cell recruitment, inflammatory reactions, suppressing oxidative stress and lipid peroxidation, rapid restoration of cellular and architectural integrity of the liver. Therefore, BM-MSCs therapy might have the upper hand in treatment of renal IRI to prevent sever remote injury that could affect severity and mortality associated with renal IRI. However, the exact mechanisms underlying the better organ recovery of liver treated with BM-MSCs in renal IRI remain to be investigated.

Study Limitations

Even though our findings are promising, molecular studies of the liver tissues were not conducted and the underlying mechanisms involved in the therapeutic effect of BM-MSCs remain descriptive. The exact role of Von-kupffer cells also remained unclear. Stem cell therapy may be promising provided assurance of safe transition to use in humans by further studies to explore whether BM-MSCs have the same hepato-protective effect in humans. Follow up after IRI looking into the chronic influence of treatment of BM-MSCs.

Conclusion

This study suggested that renal IRI initiated remote liver dysfunction and BM-MSCs enhanced morphological and functional recovery of liver as a remote organ from the renal IRI. BM-MSCs protects against remote liver injury through early inhibition of inflammatory cell recruitment, inflammatory reactions, suppressing oxidative stress and lipid peroxidation, and rapid restoration of cellular and architectural integrity of liver. This provides another important basis for the therapeutic concept of BM-MSCs in treatment of renal IRI by adding a beneficial effect on decreasing the remote liver injury besides considering it as a promising treatment in renal IRI.

Conflicts of Interest

There is no conflict of interest to declare.

Acknowledgments

I would to thank the Nile Center of Experimental Research, Mansoura, Egypt and Mr Mohamed El-Hamamy in the Pharmacology Department, Faculty of medicine, Minia University, Minia, Egypt for their technical support.

References

1. Park SW, Chen SW, Kim M, Brown KM, Kolls JK, et al. (2011) Cytokines induce small intestine and liver injury after renal ischemia or nephrectomy. *Lab Invest* 91: 63-84.
2. Thakar CV, Christianson A, Freyberg R (2009) Incidence and outcomes of acute kidney injury in intensive care units: A veteran's administration study. *Crit Care Med* 37: 2552-2558.
3. Malek M, Nematbakhsh M (2015) Renal ischemia/reperfusion injury from pathophysiology to treatment. *J Renal Injury Prevention* 4: 20-27.
4. Zhu XY, Lerman A, Lerman LO (2013) Concise Review: Mesenchymal Stem Cell Treatment for Ischemic Kidney Disease. *Stem Cells* 31: 1731-1736.
5. Golab F, Kadkhodae M, Zahmatkesh M, Hedayati M, Arab H, et al. (2009) Ischemic and non-ischemic acute kidney injury cause hepatic damage. *Kidney Int* 75: 783-792.
6. Grams ME, Rabb H (2012) The distant organ effects of acute kidney injury. *Kidney Int* 81: 942-948.
7. Serteser M, Koken T, Kahraman A, Yilmaz K, Akbulut G, et al. (2002) Changes in hepatic TNF-alpha levels, antioxidant status, and oxidation products after renal ischemia/reperfusion injury in mice. *J Surg Res* 107: 234-240.
8. Kaçmaz A, User EY, Sehirli AO, Tilki M, Ozkan S, et al. (2005) Protective effect of melatonin against ischemia/reperfusion-induced oxidative remote organ injury in the rat. *Surg Today* 35: 744-750.
9. Kadkhodae M, Golab F, Zahmatkesh M, Ghaznavi R, Hedayati M (2009) Effects of different periods of renal ischemia on liver as a remote organ. *World J Gastroenterol* 15: 1113-1118.
10. Lameire NH, Bagga A, Cruz D, De Maesseneer J, Endre Z, et al. (2013) Acute kidney injury: an increasing global concern. *Lancet* 382: 170-179.
11. Seifi B, Kadkhodae M, Najafi A, Mahmoudi A (2014) Protection of Liver as a Remote Organ after Renal Ischemia-Reperfusion Injury by Renal Ischemic Postconditioning. *International Journal of Nephrology* 4.
12. Awad A, Kamel R, Sherief M (2011) Effect of thymoquinone on hepatorenal dysfunction and alteration of CYP3A1 and spermidine/spermine N-1-acetyltransferase gene expression induced by renal ischaemia-reperfusion in rats. *Journal of Pharmacy and Pharmacology* 63: 1037-1042.
13. Hekimoglu AT, Toprak G, Akkoc H, Evliyaoğlu O, Ozekinci S (2013) Oxytocin ameliorates remote liver injury induced by renal ischemia-reperfusion in rats. *Korean J Physiol Pharmacol* 17: 169-173.
14. Kim M, Park S, Kim M, D'Agati V, Thomas H (2011) Isoflurane activates intestinal sphingosine kinase to protect against renal ischemia-reperfusion induced liver and intestine injury. *Anesthesiology* 114: 363-373.
15. Fiorina P, Jurewicz M, Augello A, Vergani A, Dada S, et al. (2009) Immunomodulatory function of bone marrow-derived mesenchymal stem cell in experimental autoimmune type 1 diabetes. *J Immunol* 183: 993-1004.
16. Lu W, Yi S, Ding J, Chen X, Zhang X (2015) Mesenchymal stem cells attenuate acute ischemia-reperfusion injury in a rat model *Experimental and Therapeutic Medicine* 10: 2131-2137.
17. Sadek EM, Affi NM, Abd Elfattah IL, Abd-El Mohsen MA (2013) Histological study on effect of mesenchymal stem cell therapy on experimental renal injury induced by ischemia/reperfusion in male albino rat. *Int J Stem Cells* 6: 55-66.
18. Sheashaa H, Lotfy A, Elhousseini F, Aziz AA, Baiomy A, et al. (2016) Protective effect of adipose-derived mesenchymal stem cells against acute kidney injury induced by ischemia-reperfusion in Sprague-Dawley rats. *Exp Ther Med* 11: 1573-1580.
19. Lange C, Tögel F, Iltlich H, Clayton F, Nolte-Ernsting C, et al. (2005) Administered mesenchymal stem cells enhance recovery from ischemia/reperfusion-induced acute renal failure in rats. *Kidney Int* 68: 1613-1617.

20. Monsel A, Zhu YG, Gennai S, Hao Q, Liu J, et al. (2014) Cell-based therapy for acute organ injury: preclinical evidence and ongoing clinical trials using mesenchymal stem cells. *Anesthesiology* 121: 1099-1021.
21. Li B, Cohen A, Hudson TE, Motlagh D, Amrani DL (2010) Mobilized human hematopoietic stem/progenitor cells promote kidney repair after ischemia/reperfusion injury. *Circulation* 121: 2211-2220.
22. Furuichi K, Shintani H, Sakai Y, Ochiya T, Matsushima K (2012) Effects of adipose-derived mesenchymal cells on ischemia-reperfusion injury in kidney. *Clin Exp Nephrol* 16: 679-689.
23. Alhadlaq A, Mao JJ (2004) Mesenchymal stem cells: isolation and therapeutics. *Stem Cells Dev* 13: 436-448.
24. Wang HJ, Varner A, AbouShwareb T, Atala A, Yoo JJ (2012) Ischemia/reperfusion-induced renal failure in rats as a model for evaluating cell therapies. *Ren Fail* 34: 1324-1332.
25. Young D (2001) *Effects of Disease on Clinical Laboratory Tests* (4th Edn) 3: 67-69.
26. Reitman S, Frankel S (1957) A colorimetric method for the determination of serum glutamic oxalacetic and glutamic pyruvic transaminases. *Am J Clin Pathol* 28: 56-63.
27. Mihara M, Uchiyama M (1978) Determination of malonaldehyde precursor in tissues by thiobarbituric acid test. *Anal Biochem* 86: 271-278.
28. Moron MS, Depierre JW, Mannervik B (1979) Levels of glutathione, glutathione reductase and glutathione S-transferase activities in rat lung and liver. *Biochim Biophys Acta* 582: 67-78.
29. Bancroft JD, Suvana S, Kim Layton C (2013) *Bancroft's Theory and Practice of Histological Techniques* China: Churchill Livingstone. Elsevier 5: 6-10.
30. El-Tahawy NF, Ali AH, Saied SR, AbdelWahab ZA (2011) Effect of glycyrrhizin on lipopolysaccharide/D-galactosamine induced acute hepatitis in albino rats: a histological and immunohistochemical study. *The Egyptian Journal of Histology* 34: 518-527.
31. Draper HH, Hadley M (1990) Malondialdehyde determination as index of lipid peroxidation. *Methods Enzymol* 186: 421.
32. Shang Y, Siow YL, Isaak CK, Karmin O (2017) Acute kidney injury induces oxidative stress and distant organ dysfunction due to glutathione depletion. *The FASEB Journal* 31 (1): 698-702.
33. Gaudio E, Onori P, Franchitto A, Sferra R, Riggio O (1997) Liver metabolic zonation and hepatic microcirculation in carbon tetrachloride-induced experimental cirrhosis. *Dig Dis Sci* 42: 167-177.
34. İşlekel H, İşlekel S, Güner G, Ozdamar N (1999) Evaluation of lipid peroxidation, cathepsin I and acid phosphatase activities in experimental brain ischemia-reperfusion. *Brain Res* 843: 18-24.
35. Bussolati B, Tetta C, Camussi G (2008) Contribution of stem cells to kidney repair. *Am J Nephrol* 28: 813-822.
36. Gruys E, Toussaint MJ, Niewold TA, Koopmans SJ (2005) Acute phase reaction and acute phase proteins. *J Zhejiang Univ Sci B* 6: 1045-56.
37. Filho MAG, Cortez E, Garcia-Souza ÉP, Soares Vde M, Moura AS, et al. (2015) Effect of remote ischemic preconditioning in the expression of IL-6 and IL-10 in a rat model of liver ischemia-reperfusion injury. *Acta Cir Bras* 30: 452-460.
38. Chapel A, Bertho JM, Bensidhoum M, Fouillard L, Young RG, et al. (2003) Mesenchymal stem cells home to injured tissues when co-infused with hematopoietic cells to treat a radiation-induced multi-organ failure syndrome. *J Gene Med* 5: 1028-1038.
39. Zhang S, Chen L, Liu T, Zhang B, Xiang D, Wang Z, Wang Y (2012) Human umbilical cord matrix stem cells efficiently rescue acute liver failure through paracrine effects rather than hepatic differentiation. *Tissue Eng Part A* 18: 1352-1364.
40. Chen YT, Sun CK, Lin YC, Chang LT, Chen YL, et al. (2011) Adipose-derived mesenchymal stem cell protects kidneys against ischemia-reperfusion injury through suppressing oxidative stress and inflammatory reaction. *J Transl Med* 5: 51.
41. Ghannam S, Bouffi C, Djouad F, Jorgensen C, Noel D (2010) Immunosuppression by mesenchymal stem cells: mechanisms and clinical applications. *Stem Cell Res Ther* 1: 2.
42. Suzuki S, Nakamura S, Sakaguchi T, Ochiai H, Konno H (1997) Alteration of reticuloendothelial phagocytic function and tumor necrosis factor-alpha production after total hepatic ischemia. *Transplantation* 64: 821-827.
43. Teoh NC, Farrell GC (2003) Hepatic ischemia reperfusion injury: pathogenic mechanisms and basis for hepatoprotection. *J Gastroenterol Hepatol* 18: 891-902.
44. Devey L, Ferenbach D, Mohr E, Sangster K, Bellamy CO (2009) Tissue-resident macrophages protect the liver from ischemia reperfusion injury via a heme oxygenase-1-dependent mechanism. *Mol Ther* 17: 65-72.